

Application of Boundary Element Method to Modelling of Added Mass and Its Effect on Hydrodynamic Forces

Paola Gardano¹ and Peter Dabnichki^{1,2}

Abstract: The work presents a numerical simulation of hydrodynamic forces generated in front crawl swimming. The three dimensional Laplace's equation is used for the analysis of the flow around a moving body in an infinite domain and considers the effect of the added mass and the acceleration on the hydrodynamic forces (Drag and Lift) generated by the interaction between the flow and the body at different geometric configurations of the arm – variable elbow angle. Boundary Element Method (BEM) was used to obtain the solution of the three dimensional equation numerically. The aim of the work was two-fold:

- 1) to investigate the effect of the added mass on the scale and trend of the forces and
- 2) to assess the suitability of BEM for obtaining reliable and accurate solution by validating the results with existing experimental data.

BEM showed robust performance as evident from the produced comparison with the experimental data and has clear advantage for this type of problem over computationally expensive computational fluid dynamics approaches.

Comparison between directly measured data from experiments on a computer controlled mechanical arm and from numerical simulation using experimentally obtained drag coefficients with the added mass correction showed clearly the significant effect of the added mass and acceleration on the magnitude and profile of hydrodynamic forces. Furthermore the result showed that the added mass effect is the main factor in propulsive force generation that explains some unexpected experimental results by Lauder and Dabnichki (2005) on the profile of the propulsive force throughout the simulated front crawl arm stroke.

keyword: Boundary Element Methods; Laplace equations; Added mass; Hydrodynamic forces.

1 Introduction

The dynamic of structures surrounded by water requires special consideration in terms of induced acceleration in water and production of extra force on the structure in addition to the fluid-dynamic drag force. This extra force can be modelled as the product of a hypothetical mass of water and the acceleration of the structure known as the added mass (Zhou Z.X., 2005). Theoretically the simplest approach for considering flow around a structure is the potential flow idealization. The surrounding water is assumed to be incompressible and non-viscous that is very close to the real behaviour of the fluid, and the resulting flow is assumed to be irrotational. The resulting governing equation under the above assumptions is the Laplace equation. However, it is evident that the imposed flow assumptions are not always correct and solutions for real-life problems need to be rigorously validated.

There have been a number of numerical studies utilising the above approach. Han and Xu (1996) presented a theoretical model of the added mass for a flexible cylinder vibrating in an irrotational and incompressible fluid medium governed by Laplace's equation. The cylinder considered slender and linearly elastic was modelled as one-dimensional beam. The added mass model was used to derive the natural frequencies of the vibrating cylinder. Carstens and Sayer (1996) developed a linear potential theory to investigate the hydrodynamic interactions between two vertical cylinders in harmonic flow. They studied the added mass effect and dampening characteristics for various cylinder diameters, length and inter-spacing. They adopted the linear diffraction theory and solved the so formulated diffraction problem by applying an integral formulation of the motion equation based on Green's theorem. Again the fluid was assumed incompressible and the flow irrotational, hence satisfying Laplace's equation. The velocity potential was split into three contributing parts, incident potential, diffracted potential and radiated potential. The diffracted one was described by a distribution of point wave sources over the

¹ Department of Engineering, Queen Mary, University of London, Mile End Road, London, E1 4NS, UK.

² Corresponding author, e-mail:p.dabnichki@qmul.ac.uk

surface of the structures. The resulting integral equations were solved by a direct numerical method. They found that the number of panels is dependent on frequency, proximity to a free-surface or other boundary, and spacing between bodies. The approach adopted in the present study was similarly based on the use of Laplace's equation to model the added mass and its effect on immersed body as the human arm represents a pseudo-cylinder.

The evaluation of the added mass effect became important in Ocean Engineering applications like the dynamic simulation of underwater vehicles (AUV), and remotely operated vehicles (ROV). Mc Millan et al. (1995) developed a dynamic simulation algorithm for an underwater vehicle (URV) with a manipulator. They modelled added mass, viscous drag, fluid acceleration and buoyancy forces. The added mass was represented by a 6×6 symmetric and positive definite matrix the derivative of the total momentum of the fluid produced a set of equations for the added mass force. This is defined as the force exerted on a rigid body accelerating through an unbounded, inviscid fluid as the fluid is not accelerating. Sahin (1995) applied the panel method (low-order singularly panel method based on Green's formulation) to hydrodynamics of underwater vehicles. The low-order modelling employs constant strength sources and doublets and the body surface is modelled by quadrilaterals. Hydrodynamic coefficients, added mass and added moment of inertia are calculated for different body shapes.

The effect of the added mass on the hydrodynamic forces during front crawl in swimming is studied in this work. Front crawl is the fastest and most effective swimming style as the arm stroke is by far the major contributor to the forward movement of the swimmer and the most important part of swimmer's propulsion. The particular problem analysed is the relative Drag and Lift forces' contribution to the propulsion and more importantly the effect of the unsteady flow condition modelled as added mass on the propulsion.

Swimming research had been until recently confined to steady analysis. Unsteady effects were introduced and analyzed in terms of kinematic data from underwater video analysis of the hand's trajectory during the swimming stroke (Lauder and Dabnichki, 2001). The applicability of the quasi-static forces values obtained by Schleihauf (1979) and Berger et al. (1995) to the unsteady conditions had already been questioned (Lauder and Dabnichki, 1996). This is in agreement with Chil-

dress (1981) where the hydrodynamic forces in swimming were described as dependent on significant unsteady effects that include vortex shedding and added mass effects. Recent experimental and theoretical studies (Lauder and Dabnichki, 2005; Gardano and Dabnichki (in press) have produced clear evidence that such effects play significant role in propulsion generation. However, due to the limitations in the experimental methods it is very difficult if not impossible to attribute the contribution of different factors to the propulsive force. Analytical approach is impossible due to the complex nature of the equations. Hence a numerical approach becomes an invaluable tool in such simulations. The most prominent such approach is the Computational Fluid Dynamics (CFD) with a variety of techniques such as Large Eddy Simulation (LES), Direct Numerical Simulation (DNS) and a variety of other less prominent methods. Although these methods are a very powerful tool in studying flow properties and type they are very intensive computationally and sometimes cumbersome for application to practical problems. Boundary Element Method (BEM) and the related Panel Method have been successfully applied to complex problems in both solid and fluid mechanics problems (Aliabadi, 2002; Qian et al. 2004, Nicolas and Bermudez, 2004; Mai-Duy and Tran-Gong, 2004, Callsen et al. 2004) and showed both computational speed and reliability.

The aim of this paper is the real estimation of the grand added mass matrix in order to show the importance of the added mass effect and the acceleration on the propulsion during the stroke. The Boundary Element Method has been adopted to find the solution of the Laplace's equation that described our potential flow problem and to calculate the added mass matrix for a model of human arm simulating front crawl-stroke in quasi-static conditions.

2 Method

The method we used to determine the added mass was a Boundary Element Method by applying the solution of the Laplace's equation that described the considered potential flow problem and through the calculation of necessary work done to change the kinetic energy associated with the motion of a fluid. We considered that a certain positive, non-zero amount of kinetic energy occurred when a body moves through a fluid.

We began our consideration by introducing an incident irrotational flow past a three-dimensional rigid body im-

mersed into a volume with surface S_∞ and that translates with velocity \bar{U} . The harmonic potential was decomposed into the incident flow that prevails in absence of the body ϕ^∞ , and the disturbance potential due to the body ϕ^D , as follows

$$\phi = \phi^\infty + \phi^D \quad (1)$$

The boundary integral representation for the disturbance component ϕ^D at a point \bar{x}_0 was

$$\begin{aligned} \phi^D(\bar{x}_0) = & - \int_B G(\bar{x}_0, \bar{x}) [\bar{U} - \nabla \phi^\infty(\bar{x})] \cdot \bar{n}(\bar{x}) dS(\bar{x}) \\ & + \int_B \nabla G(\bar{x}_0, \bar{x}) \cdot \bar{n}(\bar{x}) \phi^D(\bar{x}) dS(\bar{x}) \end{aligned} \quad (2)$$

where B denotes the body surface. The integrals over the infinite boundary surface S_∞ were infinitesimal and were not shown in the equation. Rearranging the equation (2) eliminating the single-layer potential we obtained

$$\phi(\bar{x}_0) = \phi^\infty(\bar{x}_0) - \int_B \nabla G(\bar{x}_0, \bar{x}) \cdot \bar{n}(\bar{x}) [\bar{U} \cdot \bar{x} - \phi(\bar{x})] dS(\bar{x}) \quad (3)$$

The above equation was a simplified representation for the disturbance potential in terms of a double layer potential alone.

Assuming that the point \bar{x}_0 was located sufficiently away from the body and by selecting a point \bar{x}_c in the interior or vicinity of the body we could expand the Green's function and its gradient in a Taylor series with respect to \bar{x} about the point \bar{x}_c .

$$\begin{aligned} \phi(\bar{x}_0) = & -G(\bar{x}_0, \bar{x}_c) \int_B \nabla \phi(\bar{x}) \cdot \bar{n}(\bar{x}) dS(\bar{x}) \\ & - \nabla_c G(\bar{x}_0, \bar{x}_c) \cdot \\ & \int_B [-\phi(\bar{x}) \bar{n}(\bar{x}) + (\bar{x} - \bar{x}_c) \nabla \phi(\bar{x}) \cdot \bar{n}(\bar{x})] dS(\bar{x}) + \dots \end{aligned} \quad (4)$$

The term on the right-hand side represented the flow due to a point source and its volume rate was equal to the flow rate across B . The second integral was the coefficient of the point-source dipole

$$d = \int_B [-\phi(\bar{x}) \bar{n}(\bar{x}) dS(\bar{x}) + (\bar{x} - \bar{x}_c) \nabla \phi(\bar{x}) \cdot \bar{n}(\bar{x})] dS(\bar{x})$$

$$(5)$$

Let us consider the case of a flow due to a rigid body that translating with velocity \bar{U} and rotating with angular velocity $\bar{\Omega}$ about the point \bar{x}_c . The no-penetration condition on the surface of the body required that

$$\nabla \phi(\bar{x}) \cdot \bar{n}(\bar{x}) = [\bar{U} + \bar{\Omega} \times (\bar{x} - \bar{x}_c)] \cdot \bar{n}(\bar{x}) \quad (6)$$

After a substitution of the above relation in (5), the coefficient of the dipole was expressed as

$$\begin{aligned} d = & - \int_B -\phi(\bar{x}) \bar{n}(\bar{x}) + V_B \bar{U} \\ & + \int_B \{ \bar{\Omega} \cdot [(\bar{x} - \bar{x}_c) \times \bar{n}(\bar{x})] \} (\bar{x} - \bar{x}_c) dS(\bar{x}) \end{aligned} \quad (7)$$

As clear from above the location of \bar{x}_c could be anywhere in the body and hence could be specifically chosen to coincide with the volume centre of the body. This simplified (7) considerably as the second integral term on the right hand side disappeared.

Due to the linearity of the flow governing equations and the no-penetration boundary condition, the velocity potential could be expressed as a linear combination of the translation and angular velocity about a point x_c , situated in the interior of the body, as

$$\phi(\bar{x}) = U_i(t) \Phi_i[\bar{x}, \bar{x}_c(t), \bar{e}(t)] + \Omega_i(t) \Phi_{i+3}[\bar{x}, \bar{x}_c(t), \bar{e}(t)] \quad (8)$$

Φ_i , $i = 1, \dots, 6$ were six harmonic potentials corresponding to three fundamental modes of translation and three of rotation. The vector \bar{e} described body's instantaneous orientation. The no-penetration boundary condition required that

$$\nabla \Phi_i(\bar{x}) \cdot \bar{n}(\bar{x}) = \begin{cases} n_i(\bar{x}) & i = 1, 2, 3 \\ [(\bar{x} - \bar{x}_c) \times \bar{n}(\bar{x})]_{i-3} & i = 4, 5, 6 \end{cases} \quad (9)$$

And the coefficient of the dipole in a compact form became

$$d_j = V_B (U_j + U_i \alpha_{ij} + \Omega_i \beta_{ij} + \Omega_i \gamma_{ij}) \quad (10)$$

where:

$$\alpha_{ij} = -\frac{1}{V_B} \int_B \Phi_i n_j dS \quad (11)$$

$$\beta_{ij} = -\frac{1}{V_B} \int_B \Phi_{i+3n_j} dS \quad (12)$$

$$\gamma_{ij} = \frac{1}{V_B} \epsilon_{ilk} \int_B \hat{x}_i \hat{x}_j n_k dS = -\frac{1}{V_B} \epsilon_{ijl} \int_B \hat{x}_l dV \quad (13)$$

$i, j = 1, 2, 3$, $\hat{x} = \bar{x} - \bar{x}_c$ and when x_c coincided with the centre of volume of the body the coefficients γ_{ij} vanished.

The kinetic energy for a flow generated by the motion of a rigid body was expressed as

$$\begin{aligned} K &= -\frac{1}{2} \rho \cdot \int_B \phi(\bar{x}) \bar{n}(\bar{x}) dS(\bar{x}) \\ &= -\frac{1}{2} \rho \bar{U} \cdot \int_B \phi(\bar{x}) \bar{n}(\bar{x}) dS(\bar{x}) \\ &\quad - \frac{1}{2} \rho \bar{\Omega} \cdot \int_B \phi(\bar{x}) (\bar{x} - \bar{x}_c) \times \bar{n}(\bar{x}) dS(\bar{x}) \end{aligned} \quad (14)$$

The above expressed the instantaneous kinetic energy of a potential flow in terms of a boundary integral that was a function of the distribution of ϕ over the boundary and the normal component of the velocity.

Introducing the six-dimensional vector

$$\bar{W} = (U_x, U_y, U_z, \Omega_x, \Omega_y, \Omega_z) \quad (15)$$

we defined the compact quadratic form for the kinetic energy as

$$K = \frac{1}{2} \rho V_B A_{ij} W_i W_j \quad (16)$$

where A was the six-by-six grand added matrix defined as

$$A_{ij} = -\frac{1}{V_B} \int_B \Phi_i N_j dS \quad (17)$$

with N a six-dimensional vector whose first and second three-entry blocks contained the components of the vectors n and $(\bar{x} - \bar{x}_c) \times \bar{n}$ respectively. The matrices

$$\alpha_{ij} = -\frac{1}{V_B} \int_B \Phi_i n_j dS \quad (18)$$

$$\beta_{ij} = -\frac{1}{V_B} \int_B \Phi_{i+3n_j} dS \quad (19)$$

comprised respectively the top-diagonal and bottom-left-corner three-by-three blocks of A as shown in (20) and (21)

$$A_{ij} = \begin{bmatrix} \alpha_{11} & \alpha_{12} & \alpha_{13} & \gamma_{11} & \gamma_{12} & \gamma_{13} \\ \alpha_{21} & \alpha_{22} & \alpha_{23} & \gamma_{21} & \gamma_{22} & \gamma_{23} \\ \alpha_{31} & \alpha_{32} & \alpha_{33} & \gamma_{31} & \gamma_{32} & \gamma_{33} \\ \gamma_{11} & \gamma_{12} & \gamma_{13} & \beta_{11} & \beta_{12} & \beta_{13} \\ \gamma_{21} & \gamma_{22} & \gamma_{23} & \beta_{21} & \beta_{22} & \beta_{23} \\ \gamma_{31} & \gamma_{32} & \gamma_{33} & \beta_{31} & \beta_{32} & \beta_{33} \end{bmatrix} \quad (20)$$

or in a more concise form

$$A_{ij} = \begin{bmatrix} \alpha_{ij} & \gamma_{ij} \\ \gamma_{ij} & \beta_{ij} \end{bmatrix} \quad (21)$$

From the equation of the added mass matrix was evident that the value of A depends exclusively upon the instantaneous body shape and orientation, but was independent of the body's linear or angular velocity or acceleration. Physically, A expressed the sensitivity of the kinetic energy of the fluid to the translational and rotational (angular) velocity of the moving body and may thus be regarded as an influence matrix for the kinetic energy. The matrix A was symmetric, i.e. the kinetic energy of the fluid when the body undergoes a translation along axis i and rotation about j was identical to the one generated by the body translation along j and rotation about i , with the same magnitude of the linear and angular velocities. The matrix was also positive definite, a crucial property for numerical manipulations.

Once the Added Mass matrix was obtained then the global hydrodynamic forces acting on the body directly derived. In particular the drag force (along the horizontal direction) and the lift force acting along the vertical y -axis. A combination of both forces was the propulsive force.

The computational simulation was conducted on a three dimensional model of human arm performing front crawl stroke. The arm surface mesh contained 1024 six-nodded triangular rigid spherical shell elements. To evaluate the integral at a node of a curved triangle we replaced the curved triangle with four flat triangles and perform the integration over the individual sub-elements. In this way the integral was computed accurately using a Gauss integration quadrature that is specifically designed for integration over the surface of a triangle and gives base points and weights for this geometric shape. In our specific case the number of quadrature base points was 13.

A single degree of freedom motion– rotation about the shoulder with variable speed was analysed simulating the experiment presented by Lauder and Dabnichki (2005). The kinematic variable was the angle of attack - the angle between plane of the arm (defined as the plane containing the shoulder, elbow and wrist) and the flow direction. The range of motion analysed was $0^\circ - 130^\circ$ (slightly outside the normal stroke range) in increments of 10° . The computer simulation was conducted for different arm configurations in terms of elbow flexion. The analysed configurations were for elbow angle of 180° , 160° and 135° .

The so obtained computational results were compared to the experimental ones reported by Lauder and Dabnichki (2005) obtained on a full-scale mechanical arm. The mechanical arm in their experiment was covered with a prosthetic shell and was driven about the shoulder to simulate a representative the underwater phase of a stroke similar to the front crawl stroke. A strain gauge system was used to directly measure the generated arm torque. From these data the estimated shoulder torque was calculated and compared to the direct measurement of shoulder torque from the mechanical arm. In effect the study is a computational simulation of the above study which used a direct measurement of forces generated by a robotic arm rotated in the water. This approach allows to simultaneously assess the effect of the added mass and the suitability of the BEM for use in such problems.

For the particular application the BEM showed vast superiority in both efficiency and accuracy compared to alternative numerical techniques. Alternative CFD methods require discretizing the whole of the solution domain, re-gridding the entire volume for any angle of attack, initial conditions and this considerably raises the cost of the computation. Furthermore simulation of body motion is very cumbersome as it requires constant grid modification.

3 Results

Although the potential flow at first glance seems an unrealistic approximation for the front crawl arm stroke as the arm accelerates continuously during the stroke and reaches high Reynolds numbers, the computational results were very close to the experimental ones. This suggests that the added mass effect is the dominant factor while the turbulence effect that is accounted for in the added mass as it is in the vicinity of the boundary. The

proposed numerical approach takes into account the effect of the acceleration without introducing time derivatives into the governing equation and without solving the complicated Navier-Stokes equations.

The results on Drag and Lift Forces with and without the added mass effect as obtained with the Boundary Element Method are shown below. The added mass coefficients have been multiplied by the experimentally measured acceleration as used in Lauder and Dabnichki (2005) for dynamic analysis on a mechanical arm. The graphs below (Figure 1 – 6) show the effect of the acceleration on the Drag and Lift during the front crawl stroke in swimming. As it can be seen the effect of the acceleration and the added mass is most evident in the first part of the stroke and nearly absent in the last part where the two profiles are attached with same profile.

A marked effect is more visible on the Lift profile in the first part of the stroke phase. During this initial phase the dominant force is the one perpendicular to the arm and for small angle of attack this force is equal to the Lift.

As discussed above the added mass effect has been applied to Ocean Engineering problems such as underwater vehicles, bridge piers etc. Reliable experimental results are not available and this made quite hard to demonstrate the reliability and consistency of our results. In this work used the added mass terms with given by Fossen (1995) for a prolate spheroid as this is similar shape used to approximate our model of human arm. Fossen gives these values

$$k_1 = \frac{\alpha_0}{2 - \alpha_0} \quad (22a)$$

$$k_2 = \frac{\beta_0}{2 - \beta_0} \quad (22b)$$

$$k_3 = \frac{e^4 (\alpha_0 - \beta_0)}{(2 - e^2) (2e^2 - (2 - e^2) (\alpha_0 - \beta_0))} \quad (22c)$$

where

$$\alpha_0 = \frac{2(1 - e^2)}{e^3} \frac{1}{2} \ln \left(\frac{1 + e}{1 - e} \right) - e \quad (23a)$$

$$\beta_0 = \frac{1}{e^2} - \frac{1 - e^2}{2e^3} \ln \left(\frac{1 + e}{1 - e} \right) \quad (23b)$$

and where e is the eccentricity

$$e = \left(1 - \left(\frac{D_b}{l_b} \right)^2 \right)^{1/2} \quad (24)$$

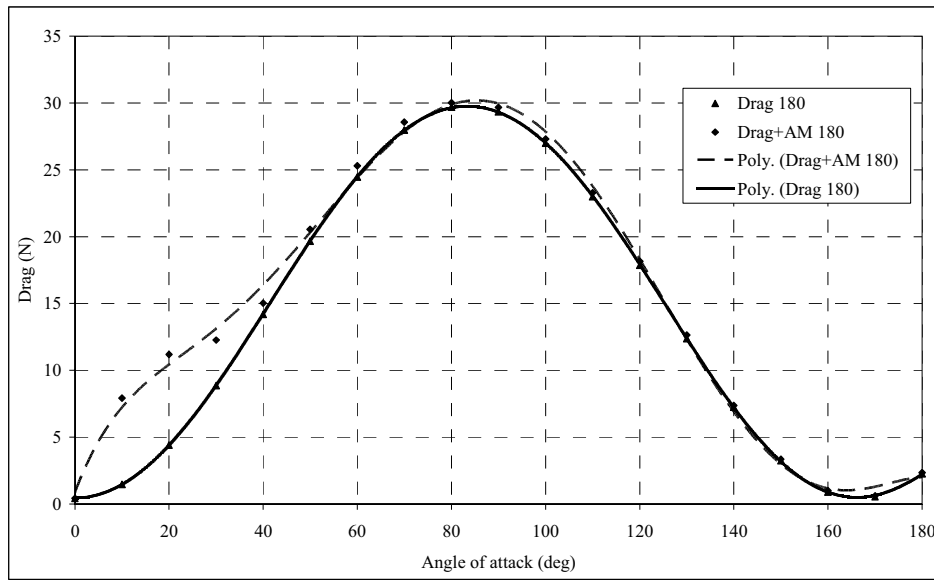


Figure 1 : Drag Force comparison to show the effect of the added mass. Elbow configuration 180⁰.

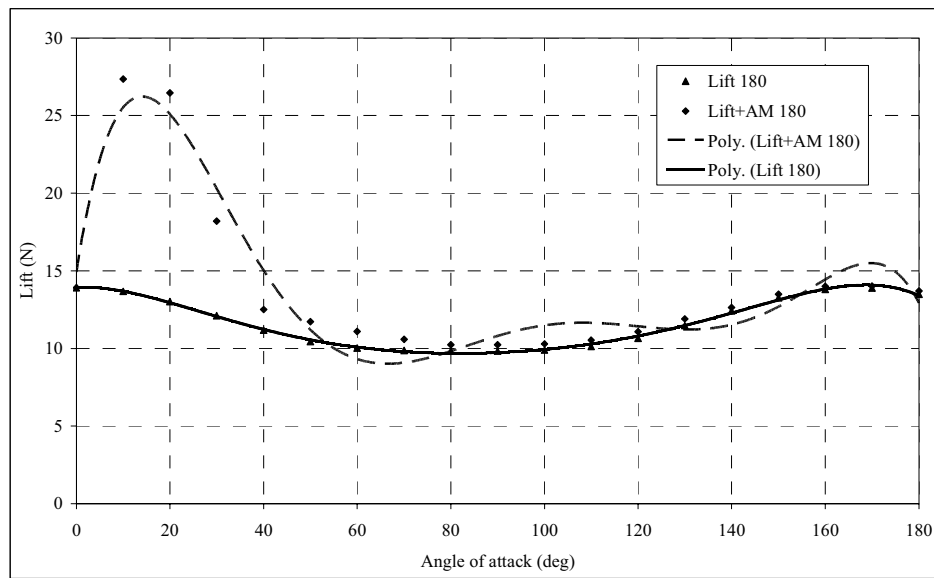


Figure 2 : Lift Force comparison to show the effect of the added mass. Elbow configuration 180⁰.

The spheroid has a minor axis of length D_b and a major axis of length l_b . Although not a prolate spheroid, the arm model can be reasonably approximated as one. In this way the Mass matrix in term of translational modes is given

$$M = \begin{bmatrix} m(1+k_1) & 0 & 0 \\ 0 & m(1+k_2) & 0 \\ 0 & 0 & m(1+k_3) \end{bmatrix} \quad (25)$$

where m is the mass of the body that in our case has been considered equal to 2.5Kg.

The values we obtained with this method are comparable with those obtained with the Boundary Element Method. The second set of results have been obtained from a calculation of the Drag and Lift as obtained from wind tunnel experiments and plus the added mass effect and compared them with the data obtained by Lauder and Dabnichki (2005) on a robotic arm simulating a front crawl

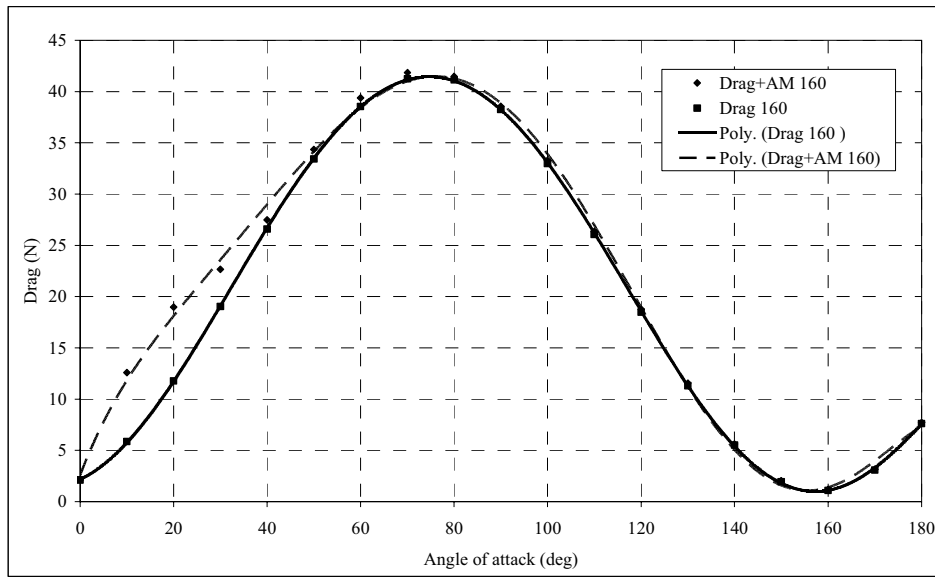


Figure 3 : Drag Force comparison to show the effect of the added mass. Elbow configuration 160°.

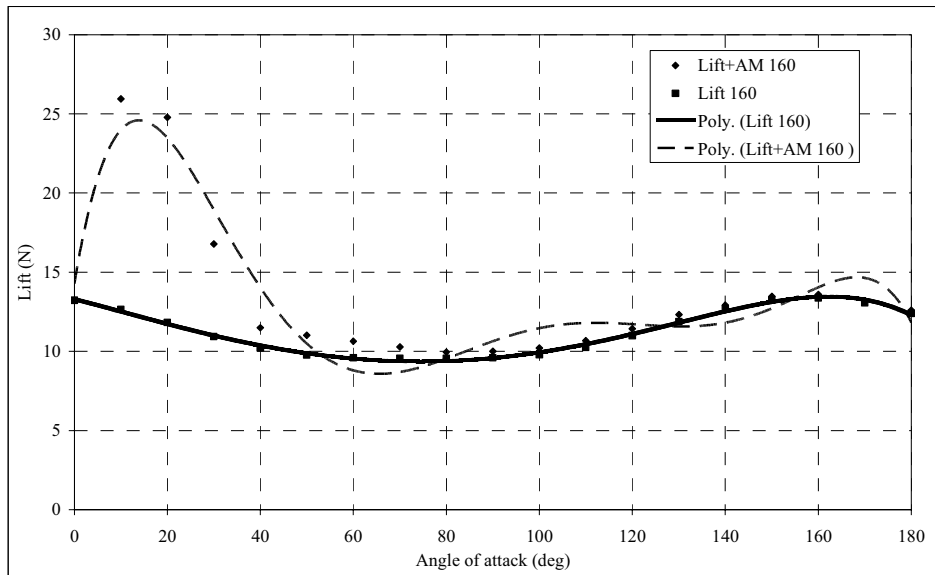


Figure 4 : Lift Force comparison to show the effect of the added mass. Elbow configuration 160°.

stroke. As can be seen from the graphs (Figure 7-9) is that the big contribution to the Torque is given by the acceleration that it's very significant in the first phase of the stroke, smaller during the central phase and nearly absent at the end of the stroke. There is a very good correspondence between the profiles in the configuration Elbow angle 180°, 160° and 135° (Figure 7, 8 and 9).

The Drag profile as obtained from the Torque divided the radius vector in case of Direct Torque and as ob-

tained from the wind tunnel experiments on the prosthetic model of human arm are presented in Figs 10, 11 and 12. Both comparisons between numerical and experimental Drag and Torque show the reliability of the selected computational approach. Furthermore one could argue that BEM has been underused in studies where the actual magnitude and profile of the hydrodynamic forces is of prime importance

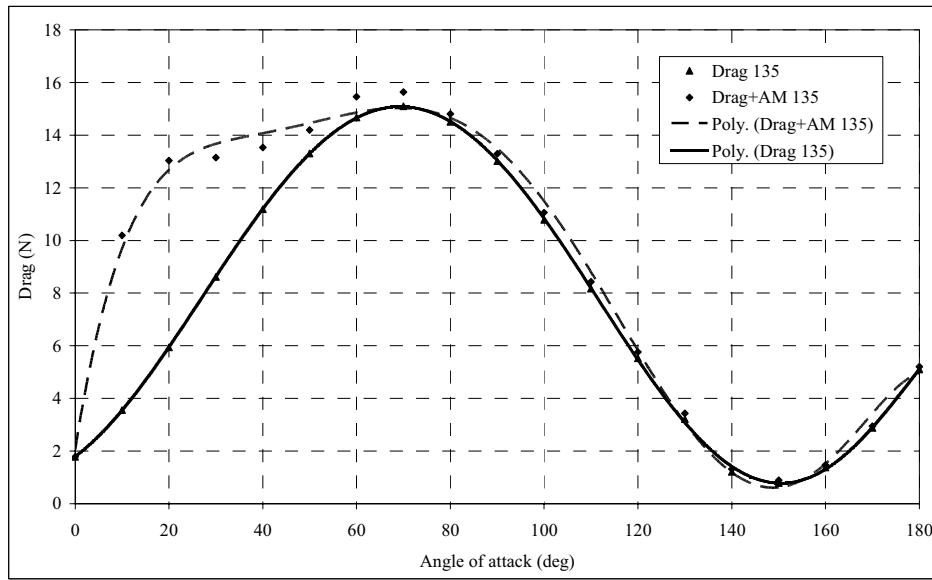


Figure 5 : Drag Force comparison to show the effect of the added mass. Elbow configuration 135⁰.

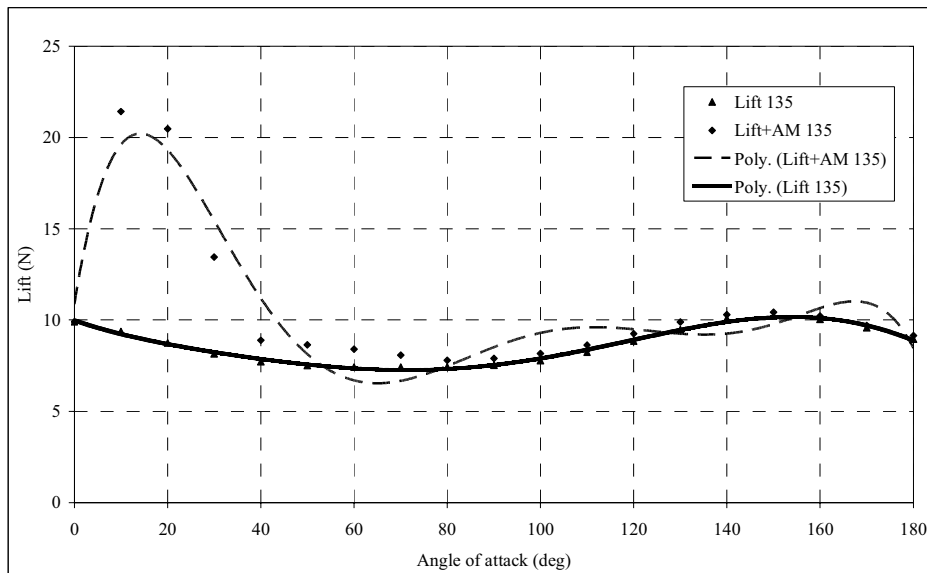


Figure 6 : Lift Force comparison to show the effect of the added mass. Elbow configuration 135⁰.

4 Conclusion

A numerical hydrodynamic model for the accelerating human arm in water at different elbow configurations was developed and tested. Three different arm configurations were analysed - elbow angle of 135⁰, 160⁰ and straight arm with elbow angle 180⁰. The added mass coefficients have been calculated using Boundary Element Method to the Laplace’s equation for the considered potential flow. In order to test the reliability of the selected numerical

implementation the obtained results were compared with those obtained with a mathematical formulation.

The presented study assessed the suitability and reliability of the Boundary Element Method to analyse the problem of the added mass. In the specific case the highly complex case of accelerating human arm was analysed and the obtained results were highly accurate as compared to the actual ones. The proposed approach could be used for numerous engineering applications related to

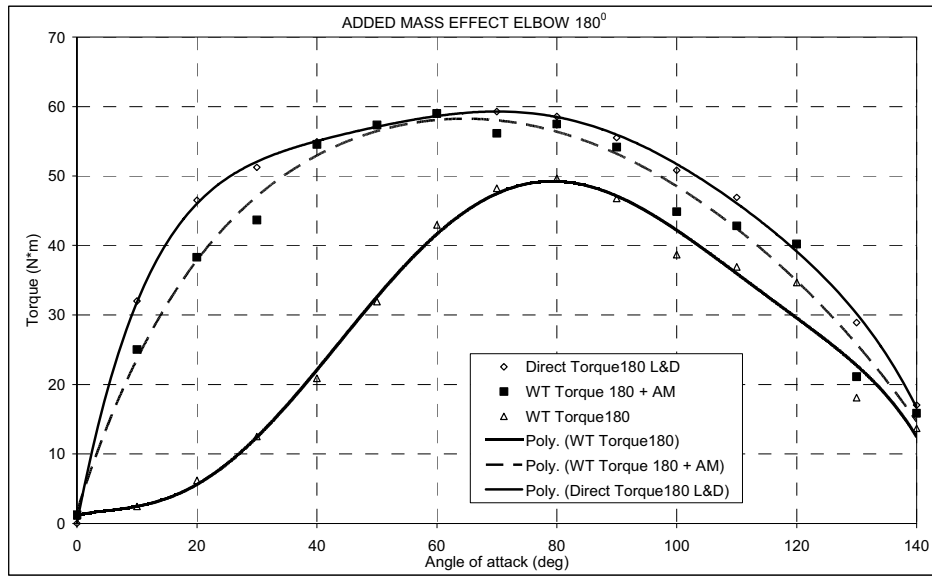


Figure 7 : Torque comparison shows the effect of the added mass. Elbow configuration 180°.

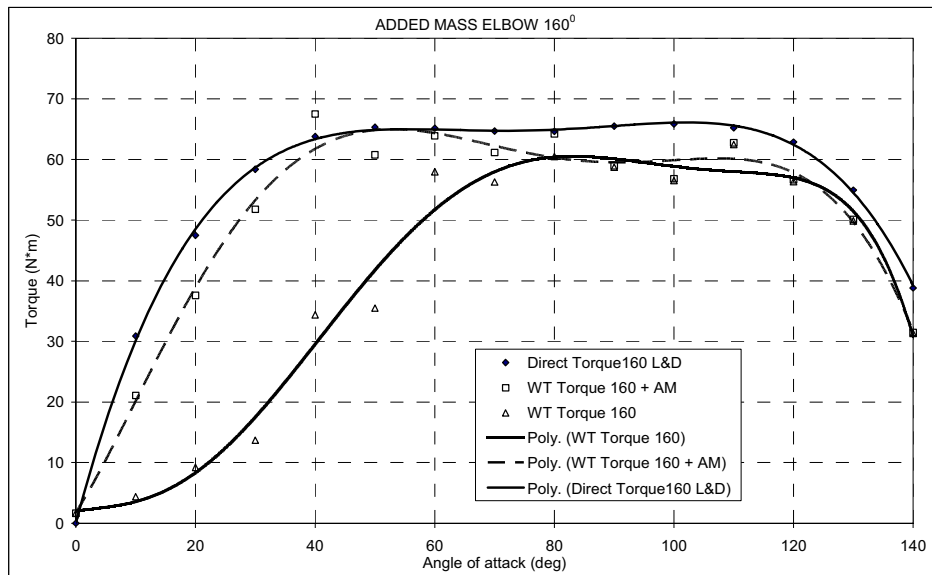


Figure 8 : Torque comparison shows the effect of the added mass. Elbow configuration 160°.

hydrodynamic forces due to body acceleration. What that makes this technique preferable to any CFD software is its simplicity, numerical stability and computational speed and accuracy. Using the Boundary Element we analyzed a potential flow and the time necessary to run the program and obtain the added mass matrix was nearly 15 sec as opposed to about 3 hours for different CFD codes. The proposed approach showed clearly that Navier-Stokes equations could be replaced with the sim-

pler as Laplace equation one, and thus avoiding the introduction the time dependency that tends to bring step depending error. Further more the lack of grid allows to fast and reliably model the body motion without the need for updating it. The approach is currently being applied to modelling of morphing structures where these superior features are becoming even more important.

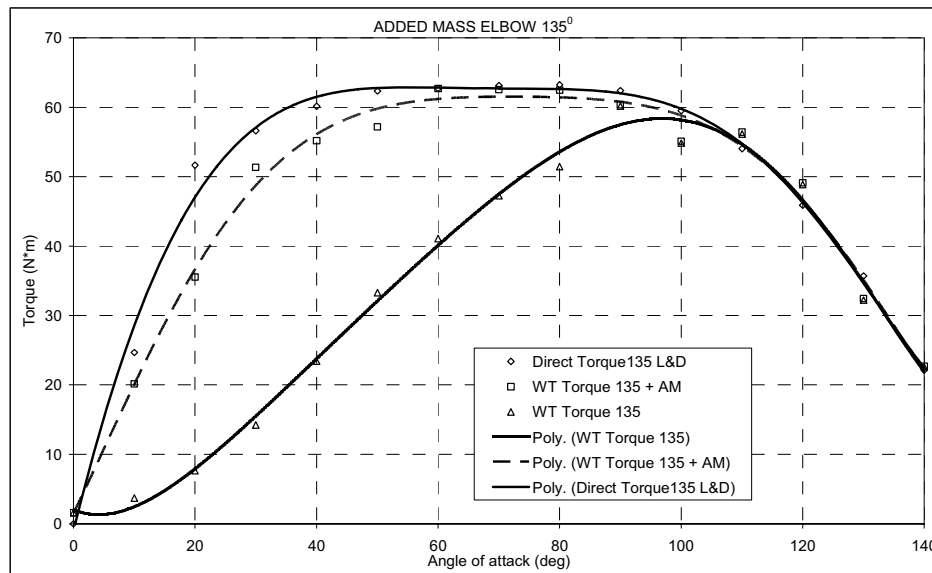


Figure 9 : Torque comparison shows the effect of the added mass. Elbow configuration 135°

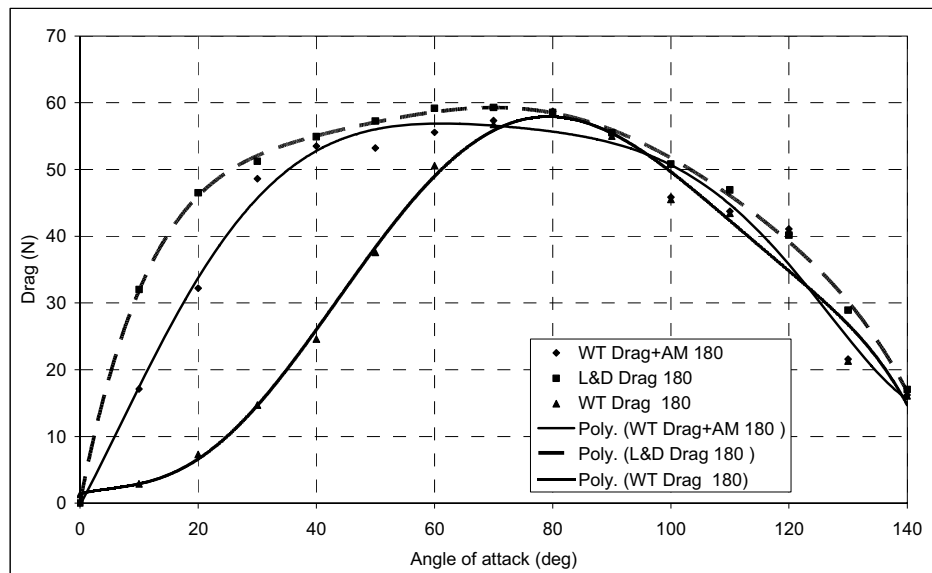


Figure 10 : Drag Force comparison to show the effect of the added mass. Elbow configuration 180°

References

Aliabadi, M. H. (2002): The Boundary Element Method. Vol. 2. Applications in solids and structures, J Wiley and Sons. Chichester.

Berger, M. A.; de Groot; G. Hollander A. P. (1995): Hydrodynamic drag and lift forces on human hand arm models. *Journal of Biomechanics*; vol. 28, pp. 125-133.

Berger, M. A. M.; Hollander A. P.; De Groot G. (1999): Determining propulsive force in front crawl swimming: A comparison of two methods. *Journal of Sports Sciences*, vol. 17, pp 97-105.

Bixler, B.; Riewald, S. (2002): Analysis of a swimmer’s hand and arm in steady flow conditions using computational fluid dynamics. *Journal of Biomechanics*, vol. 35, pp. 713-717.

Brown, R. M.; Counsilman, J. E. (1971): The role of lift in propelling swimmers. In J.M. Cooper (ed) *Biome-*

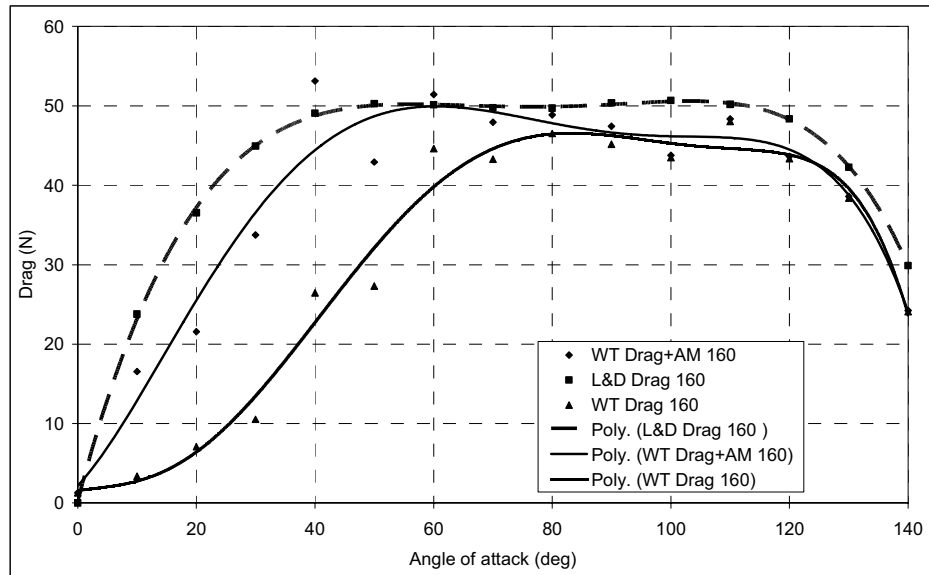


Figure 11 : Drag Force comparison to show the effect of the added mass. Elbow configuration 160⁰

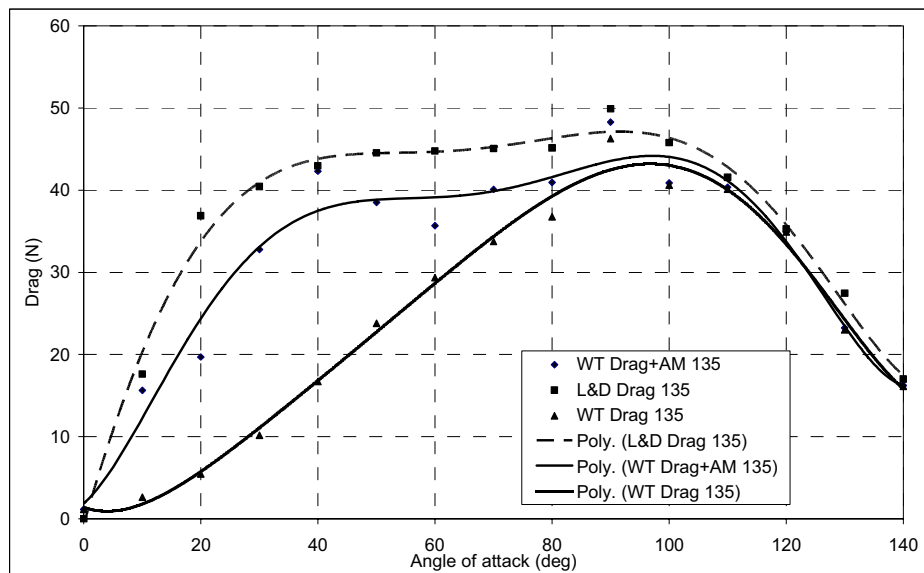


Figure 12 : Drag Force comparison to show the effect of the added mass. Elbow configuration 135⁰

chanics of Swimming, pp. 59-71.

Callsen, S.; Von Estorff, O.; Zaleski, O. (2004): Direct and indirect approach of a desingularized boundary element formulation for acoustical problems. *CMES: Computer Modeling in Engineering & Sciences* vol. 6, pp. 421-429

Carstens, B.; Sayer, P.G. (1996): Hydrodynamic interactions between two vertical circular cylinders in linear oscillatory flow. *Ocean Engineering*; vol. 24, pp. 351-

380.

Childress, S. (1981): *Mechanics of swimming and flying*. Cambridge University Press, Cambridge.

Fossen, T.I. (1995): *Guidance and control of Ocean Vehicles*. John Wiley & Sons Ltd., New York.

Gardano, P.; Dabnichki, P. (2006): On Hydrodynamics of Drag and Lift of the Human Arm, *Journal of Biomechanics*, (in press, <http://www.jbiomech.com/inpress>).

Han, R.P.S.; Xu, H. (1996): Simple and accurate added

mass model for hydrodynamic fluid-structure interaction. xx, pp. 1-17

Journal of the Franklin Institute, vol. 333B: pp. 929-945.

Lauder, M.A.; Dabnichki, P. (1996): Proposed mechanical model for measuring propulsive forces in front crawl swimming. In Steve Haake (ed) *Proceedings of the 1996 1st International Conference on the Engineering of Sport*. pp. 257-265.

Lauder, M.A.; Dabnichki, P. (2001): Improved accuracy and reliability of sweepback angle, pitch angle and hand velocity calculations in swimming. *Journal of Biomechanics*; vol. 34, pp. 31-39.

Lauder, M.A.; Dabnichki, P. (2005): Estimating propulsive forces – sink or swim. *Journal of Biomechanics*. vol. 38, pp. 1984-1990.

McMillan, S.; Orin, D.E.; McGhee, R.B. (1995): Efficient dynamic simulation of an underwater vehicle with a robotic manipulator. *IEEE Transactions on Systems, Man and Cybernetic*, vol. 25, pp. 1194-1206.

Mai-Duy, N.; Tran-Gong, T. (2004): Boundary integral-based domain decomposition technique for solution of Navier Stokes equations. *CMES: Computer Modeling in Engineering and Sciences*, vol. 6, pp. 59-75

Nicolas, A.; Bermudez, B. (2004): 2D incompressible viscous flows at moderate and high Reynolds numbers. *CMES: Computer Modeling in Engineering & Sciences*, vol. 6, pp. 441-451

Pozrikidis, C. (2002): A practical guide to the Boundary Element Method with the software library. BEMLIB.

Pozrikidis, C. (1997): Introduction to Theoretical and Computational Fluid Dynamic, Oxford University Press, Inc.

Qian, Z.Y.; Han, Z.D.; Atluri, S.N. (2004): Directly derived non-hyper-singular boundary integral equations for acoustic problems, and their solution through Petrov-Galerkin schemes. *CMES: Computer Modeling in Engineering & Sciences*, vol 5, pp. 541-562

Sahin, I.; Crane, J.W.; Watson, K.P. (1995): Application of panel method to hydrodynamics of underwater vehicles. *Ocean Engineering*, vol. 24, pp. 501-512.

Schleihauf, R.E. (1979): A hydrodynamic analysis of swimming propulsion. J. Terauds, & E.W. Bedingfield (Eds.), *Swimming II*, pp. 70-109.

Zhou Z.X.; Lo Edmond Y.M.; Tan S.K. (2004): Effect of shallow and narrow water on added mass of cylinders with various cross-sectional shapes, *Ocean Engineering*